

# The transmission characteristics of surface plasmon polaritons in ring resonator

Tong-Biao Wang, Xie-Wen Wen, Cheng-Ping Yin, and He-Zhou Wang\*

State Key Laboratory of Optoelectronic Materials and Technologies, Zhongshan (Sun Yat-Sen) University,  
Guangzhou 510275, China  
[\\*stswzh@mail.sysu.edu.cn](mailto:*stswzh@mail.sysu.edu.cn)

**Abstract:** A two-dimensional nanoscale structure which consists of two metal-insulator-metal (MIM) waveguides coupled to each other by a ring resonator is designed. The transmission characteristics of surface plasmon polaritons are studied in this structure. There are several types of modes in the transmission spectrum. These modes exhibit red shift when the radius of the ring increases. The transmission properties of such structure are simulated by the Finite-Difference Time-Domain (FDTD) method, and the eigenwavelengths of the ring resonator are calculated theoretically. Results obtained by the theory of the ring resonator are consistent with those from the FDTD simulations.

©2009 Optical Society of America

**OCIS codes:** (240.6680) Surface plasmons; (140.4780) Optical resonators; (130.7408) Wavelength filter

---

## References and links

1. W. L. Barnes, A. Dereux, and T. W. Ebbesen, "Surface plasmon subwavelength optics," *Nature* **424**(6950), 824–830 (2003).
2. H. J. Lezec, A. Degiron, E. Devaux, R. A. Linke, L. Martin-Moreno, F. J. Garcia-Vidal, and T. W. Ebbesen, "Beaming light from a subwavelength aperture," *Science* **297**(5582), 820–822 (2002).
3. D. F. P. Pile, and D. K. Gramotnev, "Plasmonic subwavelength waveguides: next to zero losses at sharp bends," *Opt. Lett.* **30**(10), 1186–1188 (2005).
4. G. Veronis, and S. Fan, "Bends and splitters in metal-dielectric-metal subwavelength plasmonic waveguides," *Appl. Phys. Lett.* **87**(13), 131102 (2005).
5. Z. Han, L. Liu, and E. Forsberg, "Ultra-compact directional couplers and Mach-Zehnder interferometers employing surface plasmon polaritons," *Opt. Commun.* **259**(2), 690–695 (2006).
6. T. Nikolajsen, K. Leosson, and S. I. Bozhevolnyi, "Surface plasmon polariton based modulators and switches operating at telecom wavelengths," *Appl. Phys. Lett.* **85**(24), 5833–5835 (2004).
7. Y. Chu, E. Schonbrun, T. Yang, and K. B. Crozier, "Experimental observation of narrow surface plasmon resonances in gold nanoparticle arrays," *Appl. Phys. Lett.* **93**(18), 181108 (2008).
8. E. Verhagen, A. Polman, and L. K. Kuipers, "Nanofocusing in laterally tapered plasmonic waveguides," *Opt. Express* **16**(1), 45–57 (2008).
9. Z. Han, E. Forsberg, and S. He, "Surface plasmon Bragg gratings formed in metal-insulator-metal waveguides," *IEEE Photon. Technol. Lett.* **19**(2), 91–93 (2007).
10. B. Wang, and G. P. Wang, "Plasmon Bragg reflectors and nanocavities on flat metallic surfaces," *Appl. Phys. Lett.* **87**(1), 013107 (2005).
11. J. Q. Liu, L. L. Wang, M. D. He, W. Q. Huang, D. Wang, B. S. Zou, and S. Wen, "A wide bandgap plasmonic Bragg reflector," *Opt. Express* **16**(7), 4888–4894 (2008).
12. A. Hosseini, and Y. Massoud, "Nanoscale surface Plasmon based resonator using rectangular geometry," *Appl. Phys. Lett.* **90**(18), 181102 (2007).
13. X. S. Lin, and X. G. Huang, "Tooth-shaped plasmonic waveguide filters with nanometric sizes," *Opt. Lett.* **33**(23), 2874–2876 (2008).
14. I. P. Kaminow, W. L. Mammel, and H. P. Weber, "Metal-Clad optical waveguides: analytical and experimental study," *Appl. Opt.* **13**(2), 396–405 (1974).
15. E. N. Economou, "Surface plasmons in thin films," *Phys. Rev.* **182**(2), 539–554 (1969).
16. A. D. Rakic, A. B. Djuricic, J. M. Elazar, and M. L. Majewski, "Optical properties of metallic films for vertical-cavity optoelectronic devices," *Appl. Opt.* **37**(22), 5271–5283 (1998).
17. I. Wolff and N. Knoppik, "Microstrip ring resonator and dispersion measurement on microstrip lines," *Electron. Lett.* **7**(26), 779–781 (1971).

## 1. Introduction

Surface plasmons are the electromagnetic surface waves that travel along the interface between metal and dielectric with an exponentially decay to the both sides. Surface plasmons polaritons (SPPs) have been considered as energy and information carriers in nanoscale optics for their ability of overcoming diffraction limit of light in conventional optics. Because of their potential applications to guide and manipulate light at deep subwavelength scales [1–3], SPPs have received plenty of attention in recent years. Several metal-insulator-metal (MIM) waveguides based on SPPs, for example, bends and splitters, Mach-Zehnder interferometers, and couplers have been designed theoretically [4–6] and demonstrated experimentally [7,8]. Some photonic band gap structures have also been proposed, such as plasmon Bragg reflectors [9], Bragg gratings with periodically varied width [10,11].

Plasmonic add/drop filters and tooth-shaped plasmonic waveguide filters have been investigated recently [12,13]. The characteristics of these filters are that many wavelengths of the light are allowed to pass through the structure while one or several wavelengths are stopped, i.e. there are one or several dips in their transmission spectra. As a matter of fact, another types of filters which only allow light at given wavelengths to transmit, while other wavelengths are forbidden, are also important in nanoscale optics. Therefore, it is necessary and meaningful to find out a SPPs filter with simple structure and whose transmission spectrum can have one or several peaks.

In this paper, we propose a two-dimensional (2D) nanoscale structure which is composed of two MIM waveguides and a ring resonator. We employ the 2D FDTD method to study the transmission characteristics of SPPs, and find that several types of modes can appear in the transmission spectrum when light passing through the structure. The wavelengths of the modes can be easily modulated by changing the radius of the ring. The eigenwavelengths of the ring have also been studied theoretically, which agrees with the FDTD simulations very well.

## 2. Theory model

It is shown in Fig. 1(a) that the 2D nanoscale structure is studied in this paper. The structure is considered invariant along  $y$  direction. The gray and white areas are silver and air, respectively. Two waveguides are coupled by a ring resonator whose outer radius is  $r_a$ , and inner radius is  $r_i$ . The radius of the ring is  $r$ , which is the average of the inner and the outer radius,  $r = (r_a + r_i)/2$ , as depicted by the dashed circle in Fig. 1(a).  $d$  are the widths of the waveguides and the ring.  $w$  are the coupling lengths between the waveguides and the ring. As is well known, the dispersion equation of SPPs in the MIM structure can be written as [14]

$$\frac{\varepsilon_0 p}{\varepsilon_m k} = \frac{1 - \exp(kd)}{1 + \exp(kd)}, \quad (1)$$

where  $k = (\beta_{gspp}^2 - \varepsilon_0 k_0^2)^{1/2}$ ,  $p = (\beta_{gspp}^2 - \varepsilon_m k_0^2)^{1/2}$ .  $\beta_{gspp}$  is the propagation constant of gap SPPs [15].  $k_0 = 2\pi/\lambda$  is the wave number of light in the air,  $\lambda$  is the wavelength of incident light.  $\varepsilon_0$  and  $\varepsilon_m$  are the dielectric functions of air and silver, respectively. For more accurately match the experimental optical constant of silver,  $\varepsilon_m$  can be characterized by the Lorentz-Drude model [16]

$$\varepsilon_m = \varepsilon_\infty - \sum_{m=0}^5 \frac{G_m \Omega_m^2}{\omega_m^2 - \omega^2 + i\omega\Gamma_m}, \quad (2)$$

where  $\varepsilon_\infty$  is the relative permittivity in the infinity frequency.  $G_m$  is the oscillator strengths,  $\Omega_m$  is the plasma frequency,  $\omega_m$  is the resonant frequency,  $\Gamma_m$  is the damping factor, and  $\omega$  is the angular frequency of incident light. All the parameters of the Lorentz-Drude model can be found in Ref [16]. Effective refraction index (ERI) of the MIM structure is defined as  $n_{eff} = \beta/k_0$ , which can be calculated by Eq. (1). Figure 1(b) shows the real part of  $n_{eff}$  as a function of

$d$  and  $\lambda$ . As seen from the figure, the  $n_{eff}$  decreases as the width  $d$  increases with the same wavelength  $\lambda$ , while  $n_{eff}$  varies very slowly when the value of  $\lambda$  changes with  $d$  fixed.

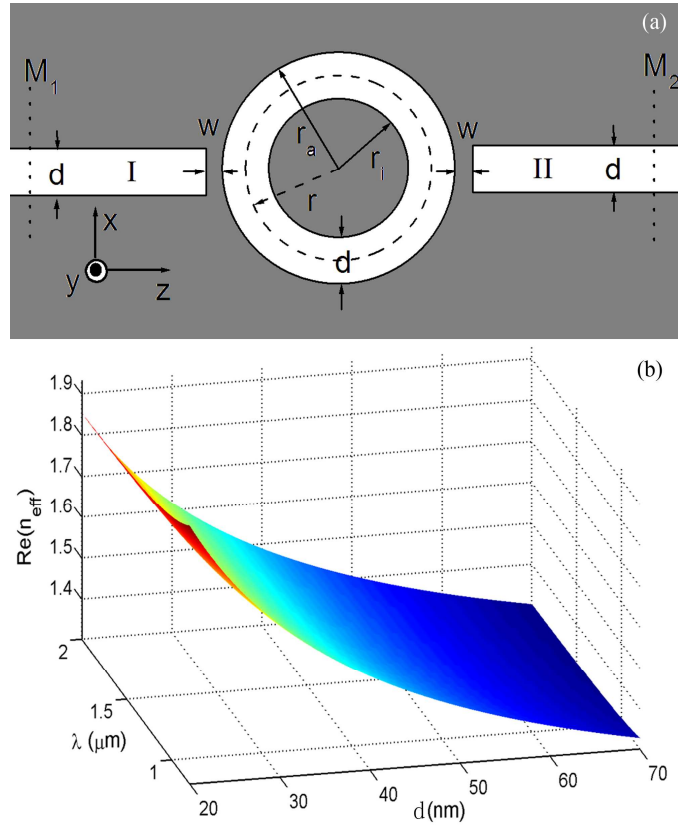


Fig. 1. (a) The structure of the nanoscale ring resonator. The gray and white areas are silver and air, respectively. (b) Dependence of  $\text{Re}(n_{eff})$  of MIM structure on the wavelength of incident light and width  $d$ .

### 3. Results and discussions

We use the 2D FDTD method with perfectly matched layer boundary conditions to simulate the transmission characteristics of SPPs. The SPPs are assumed to be excited by a dipole point source in the left side of waveguide I, and propagate along  $z$  direction. They will travel clockwise and anticlockwise simultaneously in the ring, and transmit from the right side of waveguide II. Two monitors are, respectively, put at the points of M1 and M2 to detect the incident and transmission fields for getting the incident amplitude of  $A_1$  and the transmitted amplitude  $A_2$ . The transmittance is defined to be  $T = A_2/A_1$ . Only those wavelengths satisfy the resonance condition can be transported efficiently, while others are stopped. In Fig. 2, we plot the transmission spectrum and the field distributions of the propagation of SPPs in the structure. The parameters of the structure are set to be  $d = 50$  nm,  $w = 10$  nm, and  $r = 170$  nm in calculation. One can see in Fig. 2(a), that there are three transmission peaks corresponding to the wavelength  $\lambda = 1599.2$ ,  $\lambda = 817.92$ , and  $\lambda = 579.84$  nm, respectively. Figures 2(b), 2(c), and 2(d) depict the contour profiles of fields  $|H_y|^2$  for different wavelengths. The field distributions in Figs. 2(b) and 2(d) correspond to the Modes I and II in Fig. 2(a), respectively. One can see that the SPPs can propagate through the ring, and transmit from the waveguide II for these two cases. The standing waves form in the ring at resonance. There are one and two modes in the rings of Fig. 2(b) and 2(d), respectively. It must be noted here that the wavelengths of the transmission peaks do not satisfy the simple relation  $\lambda = Ln_{eff}/N$ , where  $N$

is the mode number in the ring,  $L = 2\pi r$  is the perimeter of the ring. The resonance condition will be discussed later. In Fig. 2(c), the wavelength of the SPPs is  $\lambda = 1200$  nm. As can be seen in Fig. 2(c), the field in the ring is very weak, and almost no SPPs exist in the right-side waveguide, the transmission of SPPs is forbidden in this case.

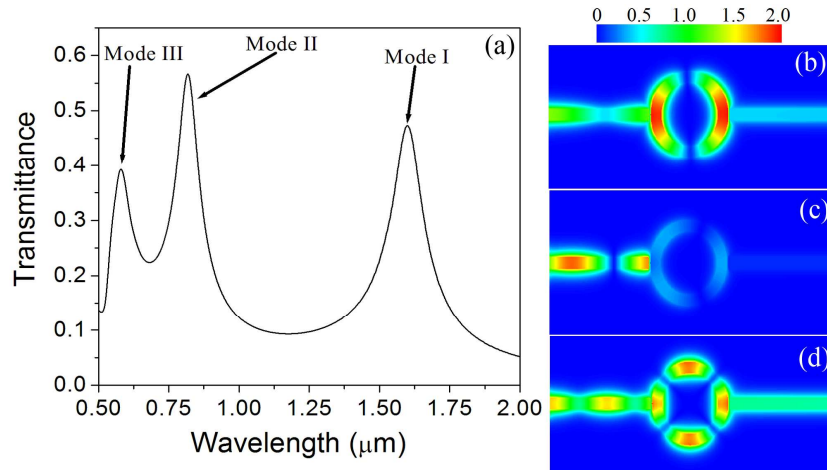


Fig. 2. (a) The transmission spectrum of the nanoscale ring resonator. The contour profiles of field  $H_y$  of the nanoscale ring resonator at different wavelengths (b)  $\lambda = 1599.2$  nm, (c)  $\lambda = 1200$  nm and (d)  $\lambda = 817.92$  nm.

Next, we would like to study the influence of the radius of the ring on the wavelengths of the transmission peaks. Figure 3 shows the transmission spectra of the SPPs for different radius of the ring. The transmission spectra plotted in black, blue, red, and green lines correspond to the rings with radii 170 nm, 180 nm, 190 nm and 200 nm, respectively. As can be seen from Fig. 3, the transmission peaks exhibit red shift as the radius increase. Since the loss of the metal is inevitable, the transmittance cannot reach 1.0. The loss will be increase when the propagation length increases.

In Fig. 4, we plot three different transmission modes as a function of radius of the ring. The horizontal coordinate is the radii of the rings, and the vertical coordinate is the corresponding wavelengths of the transmission peaks. The radius is set to vary from 100 nm to 280 nm and the interval is 10 nm in the FDTD simulations. The transmission modes for coupling length  $w = 10$  nm and  $w = 20$  nm are depicted in blue and red scattering lines, respectively. We can see that the transmission modes exhibit blue shift as the coupling length increase. Three modes are separated from each other, and intervals between them are large enough. These results will provide the theoretical basis for designing band-pass filters at the given wavelength. We will theoretically study the relationship between the wavelengths of the transmission peaks and the radii of the rings in the following.

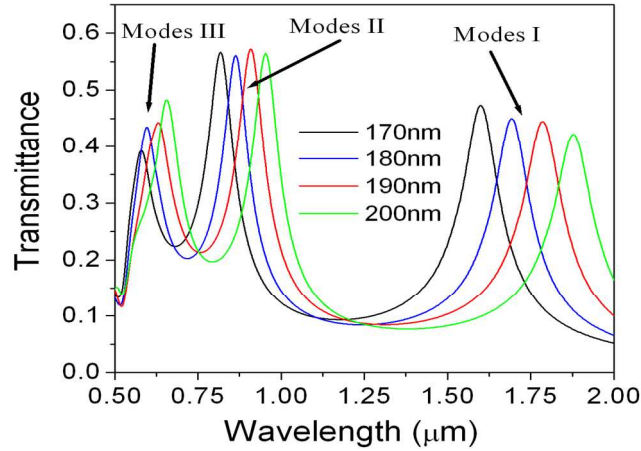


Fig. 3. Transmission spectra of the structure for different radius. The black, blue, red, and green lines correspond to the radii of 170 nm, 180 nm, 190nm, and 200 nm, respectively.

Now, we discuss the resonance condition according to the theory of ring resonator. The resonating wavelength of a ring resonator can be obtained theoretically by the following equation [17]:

$$\frac{J'_n(kr_a)}{J'_n(kr_i)} - \frac{N'_n(kr_a)}{N'_n(kr_i)} = 0, \quad (3)$$

where  $k = \omega(\epsilon_0\epsilon_r\mu_0)^{1/2}$ .  $\mu_0$  is the permeability in the air.  $\epsilon_r = n_{\text{eff}}^2 / \mu_0$  is the frequency-dependent effective relative permittivity.  $J_n$  is a Bessel function of the first kind and order  $n$ , and  $N_n$  is a Bessel function of second kind and order  $n$ .  $J'_n$  and  $N'_n$  are derivatives of the Bessel functions to the argument  $(kr)$ . Equation (3) is a transcendental equation which can be numerically solved. In principle, the ERI is wavelength dependent. However, we can see that, from Fig. 1(b), the wavelength has little influence on ERI when the width of the ring is fixed. Therefore, we can treat ERI as a constant in calculation for convenience. The real part of ERI is 1.4325 for a thickness of the waveguide of  $d = 50$  nm in the calculation, which can be obtained from Fig. 1(b). The imaginary part can be neglected because it is small and only affects the propagation length of SPPs. The calculation results are shown in Fig. 4 with black solid lines. Modes I, II, and III correspond to the one, two, and three orders of Bessel functions. One can see that there is a little difference between the theory result and the FDTD ones. In the calculation, we assume that the effective relative permittivity is the same in the whole ring, but this assumption is not exact. Since the coupling length between the ring and the waveguides are finite, the effective relative permittivity in the coupling areas is different from that in other areas of the ring. Only when the coupling length is infinite, the effective relative permittivity will be the same with that of the standard MIM model. Consequently, we can see that the FDTD results for  $w = 20$  nm are closer to the theory results than those for  $w = 10$  nm. When the radius of the ring gets larger, the effects of the coupling areas on the effective relative permittivity is smaller or even can be neglected. In addition, the curvature of the ring also have an effect on the effective permittivity, which means that for larger radius (with smaller curvature), every part of arc in the ring is closer to the straight MIM structure. Therefore, the theory results for larger radius are closer to FDTD results than that for smaller radius, which can be seen in Fig. 4. From the analysis above, we can see that the theory results match the FDTD results quite well.

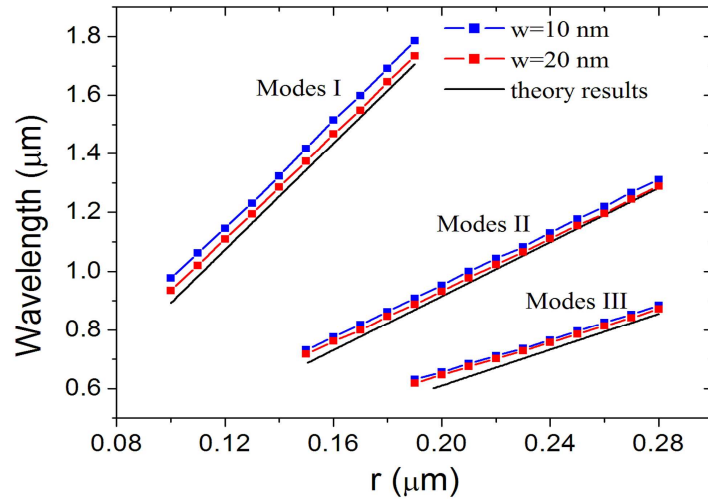


Fig. 4. The wavelengths of the transmission peaks as a function of the radius of the ring. The solid black lines are theory results; the blue and red scattering lines are FDTD results for  $w = 10$  nm and  $w = 20$  nm, respectively.

Finally, we will discuss the potential applications of our structure. Since the wavelengths of SPPs correspond to the transmission peaks are allowed to transport efficiently, while others are forbidden. Our structure can be used as SPPs band-pass filters, which is very different from the band-stop filters in previous researches. In Fig. 4, we can see that wavelengths of the peaks can vary in a considerable range (from 0.6 to 1.8  $\mu\text{m}$ ). Therefore, different types of SPPs band-pass filters can be achieved only by changing the radius of the ring. In addition, the structure is very simple and its size is very small, it also has potential applications in designing nanoscale devices.

#### 4. Conclusion

In conclusion, we have presented a novel nanoscale waveguide structure coupled by a ring resonator. The transmission characteristics of SPPs have been simulated by 2D FDTD method. The positions of transmission peaks can be easily modulated by changing the radius of the ring, which can be used to design band-pass filters for a large wavelength range. The wavelengths of transmission peaks are also calculated theoretically. The calculated results are in agreement with the FDTD results quite well. The results above imply that it have potential applications in photonics and nanoscale optics.

#### Acknowledgments

This work is supported by the National Natural Science Foundation of China (10874250, 10674183, 10804131), National 973 Project of China (2004CB719804), and Ph.D Degrees Foundation of Education Ministry of China (20060558068).